Biochimica et Biophysica Acta, 1064 (1991) 55–68

ADONIS 000527369100170Y

BBAMEM 75178

Antibodies against the 53 kDa glycoprotein inhibit the rotational dynamics of both the 53 kDa glycoprotein and the Ca^{2+}-ATPase in the sarcoplasmic reticulum membrane

James E. Mahaney [1], Christopher P. Weis [2], Charles M. Grisham [1] and Howard Kutchai [2]

[1] *Department of Chemistry, University of Virginia, Charlottesville, VA (U.S.A.) and* [2] *Department of Physiology and Biophysics Program, University of Virginia, Charlottesville, VA (U.S.A.)*

(Received 24 September 1990)
(Revised manuscript received 26 November 1990)

Key words: Glycoprotein, 53 kDa; ATPase, Ca^{2+}-; Sarcoplasmic reticulum; Saturation transfer EPR; EPR

The purpose of this study is to better define the relationship of the 53 kDa glycoprotein (GP-53) of the sarcoplasmic reticulum (SR) to other SR proteins. Towards that end the effects of antibodies against GP-53 on the rotational dynamics of maleimide spin-labeled proteins of SR of rabbit skeletal muscle were investigated. The labeling protocol used in this study provided 1.6 ± 0.3 moles spin label incorporated per 10^5 g SR protein. Labeling specificity studies indicated that nearly 70% of the label bound specifically to the Ca^{2+}-ATPase, with the remainder bound to GP-53. Using saturation-transfer electron paramagnetic resonance (ST-EPR), it was determined that the rotational mobility (i.e., the rate of rotation) of the spin-labeled SR proteins decreased greater than 5-fold upon preincubation of MSL-SR with an antiserum against the GP-53, while preincubation of MSL-SR with preimmune serum had no effect. Preincubation of MSL-SR with a monoclonal antibody against the GP-53 produced a 4-fold decrease in the rotational mobility of the MSL-SR proteins compared to control measurements. Further, these effects showed a marked calcium dependence: the decrease in the rotational mobility of the MSL-SR proteins preincubated with anti-GP-53 antibodies in 500 μM Ca^{2+} was 3–6-fold greater than that of MSL-SR preincubated with antibodies in 5 mM EGTA. While MSL was bound to both Ca^{2+}-ATPase and GP-53, model calculations indicated that the decreases observed in the rotational mobility of the MSL-SR proteins caused by the anti-GP-53 monoclonal antibodies were too large to be accounted for by effects on GP-53 alone. The calculations suggest that the rotational rate of Ca^{2+}-ATPase was also diminished by anti-GP-53 monoclonal antibodies, indicating an interaction between GP-53 and Ca^{2+}-ATPase in the SR membrane.

Introduction

The sarcoplasmic reticulum (SR) of skeletal and cardiac muscle functions to regulate the cytosolic concentration of Ca^{2+} [1,2]. The Ca^{2+}-stimulated adenosine triphosphatase, Ca^{2+}-ATPase, is an integral membrane protein of the SR membrane that is responsible for the active transport of Ca^{2+} from the cytosol to the lumen of SR at the expense of ATP. The Ca^{2+}-ATPase accounts for approximately 60–70% of the total protein of the sarcoplasmic membranes. Other major proteins include calsequestrin, a 160 kDa glycoprotein (GP-160), and a 53 kDa glycoprotein (GP-53) [3].

There is a considerable evidence that optimal Ca^{2+}-ATPase activity (i.e., Ca^{2+} transport coupled to ATP hydrolysis) is dependent on a functional interaction between individual Ca^{2+}-ATPase monomers [4–11]. This putative interaction between Ca^{2+}-ATPase monomers may be regulated or modulated by other cellular components [12]. While Ca^{2+}-ATPase isolated from cardiac muscle SR (which differs only slightly from Ca^{2+}-

Abbreviations: SR, sarcoplasmic reticulum; GP-53, 53 kDa glycoprotein of the SR; GP-160, 160 kDa glycoprotein of the SR; MAb, monoclonal antibody; ATP, adenosine 5′-triphosphate; ST-EPR, saturation transfer electron paramagnetic resonance; EGTA, ethyleneglycol bis-(β-aminoethyl ether)-*N*,*N*,*N*′,*N*′-tetraacetic acid; PMSF, phenylmethylsulfonyl fluoride; Mops, 3-(*N*-morpholino)propanesulfonic acid; Tris, tris(hydroxymethyl)aminomethane; MSL, *N*-(1-oxyl-2,2,6,6-tetramethyl-4-piperidinyl)maleimide; MSL-SR, SR labeled with MSL; DOC, deoxycholate; SDS, sodium dodecylsulfate.

Correspondence: H. Kutchai, Department of Physiology, University of Virginia Health Sciences Center, Jordan Hall, Box 449, 1300 Jefferson Park Avenue, Charlottesville, VA 22908, U.S.A.

ATPase of fast skeletal SR) is known to be regulated by phospholamban, a small multimeric membrane protein [13], it has not been established whether the Ca^{2+}-ATPase of skeletal muscle SR is regulated by any other protein. It has been suggested that GP-53 functions in this capacity [14–16], but the role of GP-53 has not been clearly defined.

The molar ratio of GP-53 to Ca^{2+}-ATPase in sarcoplasmic reticulum has been estimated to be 2:3, based on the intensity with which the two proteins stain with Coomassie blue [17]. Studies using monoclonal antibodies to localize the Ca^{2+}-ATPase and GP-53 in skeletal, cardiac, and smooth muscle have shown that the GP-53 always co-localizes with the SR-type Ca^{2+}-ATPase, whereas membranes devoid of SR-type Ca^{2+}-ATPase lack GP-53 [18].

MacLennan and co-workers [17,19] proposed that GP-53 is an intrinsic membrane protein and a major component of the SR in skeletal muscles. After further characterization, Campbell and MacLennan [19] reported that GP-53 contains a transmembrane segment with carbohydrate chains on the luminal side of the SR membrane and some of its protein mass exposed on the cytoplasmic surface of the membrane. Contrary to this finding, Leberer et al. [20] have presented evidence suggesting that GP-53 is a peripheral membrane protein associated with the luminal face of the SR membrane. Due to this conflicting data, the disposition of GP-53 relative to the SR membrane remains unresolved.

A high affinity nucleotide-binding site has been identified on the GP-53 [21], prompting the suggestion that nucleotide binding to the glycoprotein may serve to regulate its function. It has also been suggested that the GP-53 may function similarly to the β subunit of the Na, K-ATPase [15], but the finding that GP-53 has no significant sequence homology with the β subunit argues against this possibility [20].

The first evidence that GP-53 might regulate the Ca^{2+}-ATPase was reported by Chiesi and Carafoli [15] who found that the binding of trifluoperazine to GP-53 lowered the affinity of the Ca^{2+}-ATPase for Ca^{2+} and, in this way, inhibited Ca^{2+}-ATPase activity and Ca^{2+} transport.

Several groups have reported the preparation of reconstituted SR by solubilizing SR in detergent followed by detergent removal. Repke et al. [22] reported that increased KCl in the deoxycholate solubilization medium increased solubilization, but produced SR that was deficient in ATP-driven Ca^{2+} transport. Leonards and Kutchai [16] determined that KCl concentrations above 0.2 M in a cholate solubilization mixture led to a progressive decline in the amount of GP-53 present in reconstituted membranes. By varying the KCl concentration in the extraction, Leonards and Kutchai prepared reconstituted SR membranes with various levels of GP-53. In each case, the reconstituted SR had a specific activity of Ca^{2+}-stimulated ATP hydrolysis similar to native SR, but the ability of the reconstituted SR to transport Ca^{2+} declined as the amount of GP-53 in the membrane decreased. The correlation between the amount of GP-53 and the rate of ATP-dependent Ca^{2+} transport in the reconstituted preparations led Leonards and Kutchai to propose that GP-53 can modulate the coupling of Ca^{2+} transport to ATP hydrolysis by the Ca^{2+}-ATPase.

Consistent with this hypothesis, Boyd et al. [12] reported that the negative cooperativity of the dependence of Ca^{2+}-ATPase activity on ATP concentration becomes less negative as GP-53 is extracted from SR or when SR is incubated with antiserum against GP-53, and that the positive cooperativity of the dependence of Ca^{2+}-ATPase activity on the free Ca^{2+} concentration is diminished as GP-53 is extracted from SR or SR is treated with antiserum against the GP-53.

Kutchai and Campbell [14] preincubated SR with antibodies against GP-53. They found that treating SR with an anti-GP-53 antiserum caused a decline in ATP-driven Ca^{2+} transport, while Ca^{2+}-stimulated ATPase activity was unaffected. Preincubation of SR with two monoclonal antibodies against GP-53 had no effect on either Ca^{2+} transport or Ca^{2+}-ATPase activity and treatment of SR with a monoclonal antibody against the Ca^{2+}-ATPase also had no effect on either Ca^{2+} transport or Ca^{2+}-ATPase activity. However, when SR was treated with either monoclonal antibody against GP-53 concurrently with the monoclonal antibody against Ca^{2+}-ATPase, the rates of Ca^{2+} uptake and ATP hydrolysis declined proportionally. The results are consistent with the interpretation that GP-53 can modulate the function of the Ca^{2+}-ATPase in the SR membrane. Kutchai and Campbell suggested that the simultaneously bound antibodies might uncouple Ca^{2+} transport from ATP hydrolysis by sterically disrupting an interaction between GP-53 and the Ca^{2+}-ATPase required for optimal coupling. The validity of this interpretation requires a physical interaction between GP-53 and the Ca^{2+}-ATPase in the SR membrane, which can be modified by antibody binding.

In this paper, studies designed to test whether there is a physical interaction between the 53 kDa glycoprotein and the Ca^{2+}-ATPase in the SR membrane are presented. Preincubation of SR with antibodies against GP-53 retarded the rotational mobility of spin-labeled SR proteins (i.e., Ca^{2+}-ATPase and GP-53). Spectral simulations indicated that the decrease in rotational mobility of the SR proteins induced by an anti-GP-53 monoclonal antibody was too great to be accounted for by antibody effects on GP-53 alone. This suggests that the rotational mobility of Ca^{2+}-ATPase was also diminished by the anti-GP-53 monoclonal antibody, supporting the interpretation that GP-53 and Ca^{2+}-ATPase interact.

Methods

Materials

Sucrose, $CaCl_2$, KCl, and glycerol were obtained from Mallinckrodt. Benzene was obtained from Fisher Scientific. Mops, TrisCl, ATP, oxalic acid, EGTA, PMSF, maleic acid, deoxycholate, [2,3-^{14}C]maleic anhydride and bovine hemoglobin were obtained from Sigma Chemical Company. Maleimide spin label was obtained from Aldrich Chemical Company. $^{45}CaCl_2$ was obtained from New England Nuclear. In each case, materials used were of the highest purity available.

Preparation and characterization of sarcoplasmic reticulum

Light sarcoplasmic reticulum (SR) was prepared by the method of Eletr and Inesi [23] and stored at −70°C in 0.88 M sucrose in 10 mM Mops (pH 7.0). The rate of Ca^{2+}-stimulated ATP hydrolysis by SR vesicles was estimated by an enzyme-coupled assay as previously described [16,24]. The rate of ATP-driven uptake of $^{45}Ca^{2+}$ by SR vesicles was determined in the presence of oxalate using Millipore filters to trap the Ca^{2+}-loaded vesicles [14,25]. Protein concentrations were determined by the method of Lowry et al. [26].

Spin labeling sarcoplasmic reticulum with maleimide spin label

The procedure used for spin labeling sarcoplasmic reticulum (SR) was adapted from Yamada and Ikemoto [27]. SR (3 mg/ml) was added to a buffer containing 0.2 M sucrose, 1 mM EGTA, 0.97 mM $CaCl_2$, 50 mM Tris-maleate (pH 7.0). MSL (1 mM final) was added to the SR mixture and allowed to react for 12 min at room temperature. The reaction was stopped by dilution of the mixture into 20 ml of ice-cold 0.1 M KCl, 20 mM Mops (pH 7.0), and unbound label was removed by washing the membranes twice in this buffer by centrifugation at $100000 \times g$ for 50 min at 4°C. The final pellet was resuspended to 5–10 mg/ml in 0.1 M KCl, 0.2 M sucrose, 20 mM Mops (pH 7.0), and stored at −20°C until use.

Synthesis of ^{14}C-MSL

The ^{14}C-containing nitroxide derivative of *N*-ethylmaleimide (MSL) was synthesized according to Griffith and McConnell [28]. The radioisotope was introduced into the spin label by using 250 μCi of [2,3-^{14}C]maleic anhydride in the synthesis. The final ^{14}C-MSL product was purified by recrystallization in benzene. The purity of the label was checked by thin-layer chromatography which indicated predominantly ^{14}C-MSL with a small amount of spin-labeled ^{14}C-isomaleimide. The radioactivity of the label was measured in a scintillation counter, and the nitroxide content was evaluated by EPR. The final product contained 58.3 μCi/mmol spin label.

Purification of GP-53 from SR

The 53 kDa glycoprotein was purified from SR according to Campbell and MacLennan [19] using a Con-A-Sepharose 4B affinity column equilibrated with 150 mM KCl, 2.5 mg/ml deoxycholate (DOC), 10 mM Tris (pH 8.0). SR (25 mg/ml) was incubated in 1 M KCl, 10 mM Tris (pH 8.0) and DOC was added slowly to a final concentration of 0.1 mg DOC/mg SR. The DOC-extracted SR was pelleted by centrifugation at $100000 \times g$ for 45 min at 4°C. The supernatant was collected and loaded onto the equilibrated Con-A column. The extracted glycoproteins were eluted with 10 mg/ml DOC in 150 mM KCl, 0.5 M methyl α-D-mannopyranoside, 10 mM Tris (pH 8.0). The eluate was collected and dialyzed against 10 mM Tris (pH 8.0) and the composition of the eluate was evaluated by gel electrophoresis [29].

Incubation of MSL-SR with antibody preparations

The anti-GP-53 antiserum and preimmune serum were generous gifts of Dr. David H. MacLennan of the University of Toronto [30]. The monoclonal antibodies (MAbs) used in these experiments were kindly provided by Dr. Kevin P. Campbell, University of Iowa [31]. The antibody preparations we used were: (1) an antiserum produced in sheep against purified GP-53, (2) mouse ascites fluid containing MAb XB52 against the GP-53, (3) mouse ascites fluid containing MAb VIE8 against the Ca^{2+}-ATPase, and (4) mouse ascites fluid containing MAb VIII8D12 against calsequestrin.

Media for preincubation of MSL-SR with antiserum or with ascites fluid containing monoclonal antibodies contained MSL-SR (2–3 mg/ml) in 0.1 M KCl, 50 μM $CaCl_2$, 100 mM sucrose, 200 μM phenylmethylsulfonyl fluoride (PMSF), 5 mM Mops (pH 7.0). The amount of antibody preparation added to the incubation mixture (measured in μl/mg MSL-SR) depended on the particular antibody preparation used. MSL-SR was preincubated with the antibody preparation for 2 h at room temperature, unless otherwise specified. The membranes were then diluted into 20 ml 100 mM KCl, 20 mM Mops (pH 7.0), pelleted by centrifugation at $100000 \times g$ at 4°C for 50 min, and resuspended in 150 μl of 0.1 M KCl, 50 μM $CaCl_2$, 100 mM sucrose, 5 mM Mops (pH 7.0).

A. Volume tirations of MSL-SR with antibodies. MSL-SR (3 mg/ml) was incubated in 0.1 M KCl, 50 μM $CaCl_2$, 100 mM sucrose, 200 μM PMSF, 5 mM Mops (pH 7.0) with various volumes of antiserum or ascites fluid. Incubation conditions are specified in the corresponding figure legends. Following the incubation, the samples were washed as outlined above, and prepared for EPR as described below. Control incubations of either MSL-SR alone or MSL-SR incubated with various volumes of preimmune serum were carried out in the same way.

B. Titration of MSL-SR with MAb VIE8 (anti-Ca^{2+}-ATPase). Three samples of MSL-SR were prepared as above and 50, 100, 200 μl ascites containing VIE8/mg MSL-SR were added, respectively. The samples were incubated 18 h at 4 C, diluted into 20 ml 100 mM KCl, 20 mM Mops (pH 7.0), and pelleted by centrifugation at 100000 × *g* at 4°C for 50 min. The pellets were resuspended in 150 μl of 0.1 M KCl, 50 μM $CaCl_2$, 100 mM sucrose, 5 mM Mops (pH 7.0).

C. Time titration of MSL-SR with antibodies. Six samples of MSL-SR (2 mg each, 1 ml final volume) in 0.1 M KCl, 50 μM $CaCl_2$, 100 mM sucrose, 200 μM PMSF, 5 mM Mops (pH 7.0) were prepared and 10 μl antibody preparation per mg MSL-SR was added to each sample. The six samples were incubated at 4°C for 6, 12, 18, 24, 36, and 48 h, respectively, then washed with a single centrifugation. Control samples of MSL-SR incubated either alone or with 10 μl preimmune serum were prepared in a similar fashion.

Calcium dependence of antibody effects on MSL-SR

For calcium-dependence experiments, the incubation medium for antibody binding was modified to contain 0.1 M KCl, 200 mM sucrose, 200 μM PMSF in 20 mM Mops (pH 7.0) with either 500 μM $CaCl_2$ for the calcium containing incubations, or 5 mM EGTA for the calcium-free incubations. Six experiments were performed, both in calcium-containing and calcium-free antibody binding medium. These were (1) control experiment with MSL-SR alone, (2) control experiment of MSL-SR with 10 μl preimmune serum/mg MSL-SR, (3) MSL-SR with 10 μl antiserum/mg MSL-SR, (4) MSL-SR with 100 μl ascites containing XB52/mg MSL-SR, (5) MSL-SR with 100 μl ascites containing VIE8/mg MSL-SR, and (6) MSL-SR with 50 μl ascites containing VIIID-12 (an MAb against calsequestrin) per mg MSL-SR. Duplicate samples were incubated either with our without calcium for 18 h at 4°C. Following incubation, samples containing calcium were centrifuged and resuspended in 150 μl of 0.1 M KCl, 500 μM $CaCl_2$, 20 mM Mops (pH 7.0) while the samples without calcium were centrifuged and resuspended in 150 μl of 0.1 M KCl, 5 mM EGTA, 20 mM Mops (pH 7.0).

Spin labeling of hemoglobin with maleimide spin label

Maleimide spin-labeled hemoglobin was prepared according to Hemminga et al. [32]. Bovine hemoglobin (Sigma) was dissolved in 100 mM sodium phosphate (pH 6.8) to 100 mg/ml. MSL was added to the hemoglobin solution to 6 mM and allowed to react overnight at 4°C. Unreacted MSL was removed from the mixture by extensive dialysis against 100 mM sodium phosphate (pH 6.8) at 4°C, for 24–48 h or until the conventional EPR spectrum of the spin-labeled hemoglobin (MSL-Hb) solution showed no free label. The MSL-Hb solution was concentrated to 300 mg/ml using an Amicon Centricon 30 microconcentrator and stored at 4°C until use.

Preparation of MSL-SR samples for EPR measurements

MSL-SR samples were prepared for EPR by pelleting the membranes a final time by centrifugation at 100000 × *g* for 10 min at 4°C in a Beckman Airfuge. Excess buffer was siphoned off of the pellet, and the sample was homogenized in the airfuge tube with a small glass rod. Samples prepared in this fashion were reproducibly 45–50 mg/ml.

EPR samples were contained in a special, gas-permeable capillary made of the methylpentene polymer, TPX, described by Popp and Hyde [33]. The TPX capillary used in this work was kindly provided by Dr. David Thomas of the University of Minnesota. The homogenized pellet was drawn into the capillary by gentle suction, and enough was drawn into the capillary such that the sample length was 20 mm [34]. The TPX tube seated directly into a small Teflon plug that rested on the variable temperature cavity dewar sample stops, and a larger Teflon plug which extended above the sample and out of the dewar. The TPX tube and Teflon holders were held in the concentric center of the cavity using a delrin cap shim, which was notched to allow free flow of cooled N_2 gas over the assembly. The seating pieces were sufficiently small to that only the sample entered the cavity. Special marks on the sample holder, the cavity and the magnet were used to verify correct and consistent placement of the holder in the cavity.

Spin labeled hemoglobin EPR sample preparation

MSL-Hb samples used in the collection of reference spectra were 45 mg/ml hemoglobin dissolved in glycerol-water mixtures of 70%, 80%, 85%, 90%, and 95% (v/v). To collect a reference spectrum corresponding to no motion (rigid limit), a small amount of Hb-MSL was mixed with unlabeled hemoglobin and lyophilized as described by Thomas et al. [35]. All hemoglobin samples were contained in sealed quartz capillaries, which were mounted in the Teflon holders (described above) during EPR analysis. The samples were stored in their capillaries at −20°C when not in use.

EPR instrumentation

All conventional and saturation transfer EPR (ST-EPR) experiments were performed using a Varian E-109 Century Series X-band spectrometer with an E-231 cavity (TE_{102} mode) with temperature control provided by a Varian E321 cavity dewar insert equipped with a heater-sensor probe. Conventional (V_1) spectra were recorded using a non-saturating microwave field (H_1) of 0.032 gauss, a 100 gauss scan range, 100 kHz modula-

tion frequency with 2 gauss peak-to-peak modulation amplitude, and 100 kHz detection. Saturation transfer (V_2') spectra were recorded using a saturating H_1 of 0.25 gauss, a 100 gauss scan range, 50 kHz field modulation with 5 gauss peak-to-peak modulation amplitude, and 100 kHz detection set 90° out-of-phase. Proper adjustment of the incident microwave power to produce specific H_1 values was carried out according to Squier and Thomas [36] as was proper adjustment of the receiver phase to the true in-phase or out-of-phase condition. The modulation field amplitude, H_m, of the EPR spectrometer was calibrated according to Hemminga et al. [34]. Spectra were digitized as 1000 points and stored on floppy disks with an AT&T 6300 PC using an IBM-compatible software/interface package developed by Morse [37].

ST-EPR reference spectra and construction of standard curves

Rotational correlation times for ST-EPR spectra were determined using reference spectra from a model system for which correlation times can be calculated from viscosity, temperature, and structural data [35]. Standard spectra were obtained using maleimide spin-labeled hemoglobin (MSL-Hb). Rotational correlation times for MSL-Hb were calculated using the Debye equation assuming Brownian rotational diffusion [35]

$$\tau_r = 4\pi\eta R^3/3kT \quad (1)$$

where η is the solvent viscosity, k is the Boltzmann constant, T is the absolute temperature, and R is the effective radius of the hydrated protein. The spherical radius of Hb-MSL used in the calculations was 29 Å, and the viscosities of the aqueous glycerol solutions were obtained from Segur and Oberstar [38]. For each of the reference samples, conventional and saturation transfer spectra were collected at various temperatures, yielding a full series of reference spectra with rotational correlation times in the range 10^{-3} s $< \tau_r < 10^{-7}$ s (see Fig. 2, Ref. 36).

The ST-EPR model spectra were quantified using the high-field lineheight ratio, H''/H [36]. This ratio was obtained by measuring the spectral peak height near the high-field turning point (H) and the spectral height 10 gauss downfield (H''). Both heights were measured from the baseline. The dependence of H''/H on τ_r for the MSL-Hb samples served as the standard curve for determining τ_r from H'/H ratios for all experimental samples.

Experimental ST-EPR spectra

ST-EPR spectra of MSL-SR were obtained as described above, and for each spectrum, the high-field lineheight ratio was determined. Noise in the high-field region of V_2' spectra induced errors in accurately measuring the lineheights H and H'' at their distinct positions in the spectra. Therefore, the following procedures were used: (1) the spectral lineheight corresponding to H'' was determined by averaging the spectral lineheight of each data point over a 2 gauss window of the spectrum centered on H'' and (2) the spectral lineheight corresponding to H was determined by fitting the high-field peak over a 1 gauss window centered on H using a second order polynomial peak fitting program developed by Robert L. H. Bennett of the University of Minnesota. This peak fitting program was kindly made available for this analysis by Dr. David D. Thomas of the University of Minnesota. For each V_2' spectrum, H''/H errors arose from the noise uncertainty in H'', which translated into standard deviations of τ_r. For repeated experiments, errors in the ratio H''/H were tabulated as standard deviations of H''/H for n experiments, which also translated into standard deviations of τ_r.

Results

Development of procedure to spin label the Ca^{2+}-ATPase

The protocol used to label the Ca^{2+}-ATPase was adapted from the method of Yamada and Ikemoto [27] designed to label a single sulfhydryl group specifically on the Ca^{2+}-ATPase while preserving full ATPase activity coupled to Ca^{2+} transport. We chose not to block fast reacting sulfhydryl groups with *N*-ethylmaleimide before binding maleimide spin label since this can induce a loss of Ca^{2+}-ATPase activity [27,39]. SR was incubated with MSL in the presence of 0.97 mM $CaCl_2$, buffered by 1 mM EGTA for 12 min at room temperature. Unbound label was removed by washing the SR twice in 0.1 M KCl, 20 mM Mops (pH 7.0) by centrifuging the membranes at $100000 \times g$ for 50 min at 4°C. SR pellets were resuspended to 5–10 mg protein/ml in 0.1 mM KCl, 0.2 M sucrose, 20 mM Mops (pH 7.0). The maleimide spin-labeled SR (MSL-SR) produced by this method had 1.6 ± 0.3 spin labels per 10^5 g SR protein.

To determine the effects of the spin-labeling procedure on the functional state of Ca^{2+}-ATPase the SR vesicles, we determined the Ca^{2+}-ATPase activity and the rate of ATP-driven Ca^{2+} uptake before and after spin labeling. The spin-labeling procedure produced no significant decrease in either Ca^{2+}-ATPase activity or Ca^{2+} uptake. Fig. 1 shows the kinetics of accumulation of Ca^{2+} by SR vesicles before and after labeling with MSL, at 25°C. These results indicate that labeling Ca^{2+}-ATPase with MSL to the limited extent attained in these experiments does not significantly denature the Ca^{2+}-ATPase or alter its transport or enzymatic functions and that the labeling procedure does not cause the SR membrane to become leaky to Ca^{2+}.

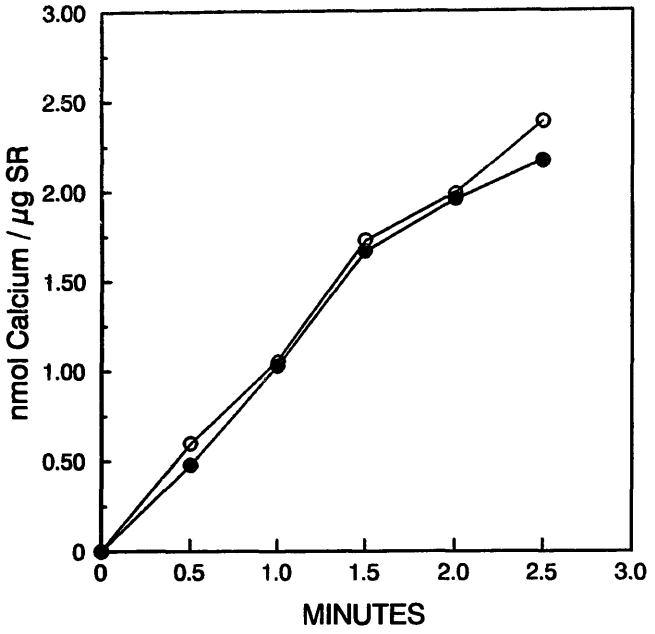

Fig. 1. Calcium uptake by MSL-SR at 25° C. SR vesicles were labeled with MSL as described in Methods [27], then ATP-driven ^{45}Ca uptake was determined [14]. For measurement of ^{45}Ca uptake, about 16 μg of SR or MSL-SR protein was added to 2.925 ml of assay mix, 0.5 ml were removed for blanks, and then uptake initiated by adding 75 μl of 0.1 M ATP. The assay mix contained 100 mM KCl, 50 mM histidine (pH 6.8), 6 mM potassium oxalate, 3 mM $MgCl_2$, and 50 μM $^{45}CaCl_2$ (2 mCi/mmol). At the times indicated, 200 μl samples were filtered on 25 mm HA Millipore filters and the filters washed twice with 4 ml of ice-cold Tris-buffered saline. Data shown present control SR (open cicles) and MSL-SR (filled circles).

Labeling specificity

The labeling stoichiometry indicated that more than one mole of spin label was incorporated per mole of Ca^{2+}-ATPase. Since the Ca^{2+}-ATPase and the 53 kDa glycoprotein together contain all of the reactive sulfhydryl groups accessible on the extravesicular side of the SR membrane [39,40], we sought to determine if the labels incorporated into the SR were bound exclusively to the Ca^{2+}-ATPase.

(1) Gel electrophoretic separation of MSL-labeled proteins. MSL-SR membranes were subjected to SDS gel electrophoresis [29]. The resulting protein bands were then analyzed for the presence of MSL. This was done either by excising the bands and analyzing them by conventional EPR spectroscopy or by autoradiography of gels of SR labeled with ^{14}C-MSL. We synthesized the ^{14}C-MSL [28], which had a specific activity of 58.4 μCi/mmol. In both types of experiments we failed to detect MSL associated with any protein band of the SDS-polyacrylamide gel. It appears that the linkage of MSL to SR proteins was cleaved under the reducing conditions of the gel electrophoresis.

(2) Detergent extraction of GP-53 and separation from Ca^{2+}-ATPase on Con-A-Sepharose. SR was spin-labeled in the normal fashion and the 53 kDa glycoprotein (GP-53) was extracted with deoxycholate and purified on a Con-A-Sepharose column as described by Campbell and MacLennan [19]. There were two fractions collected: the column void volume, which contained predominantly Ca^{2+}-ATPase and a small amount (< 5%) of calsequestrin, and the α-methylmannoside eluate, which contained predominantly GP-53 (> 90%) with a small amount of GP-160. The protein composition of these fractions was analyzed by gel electrophoresis. EPR analysis of both fractions indicated the presence of bound, strongy immobilized, spin label, indicating that in addition to labeling the target Ca^{2+}-ATPase, MSL had also bound to GP-53. Our results indicated a labeling stoichiometry of 1.3 ± 0.1 moles MSL bound per mole of Ca^{2+}-ATPase and 0.9 ± 0.1 mole MSL bound per mole of glycoprotein. Given 3 Ca^{2+}-ATPase molecules for every 2 GP-53 [17], then 68.4% of the total intensity in the EPR spectra arose from MSL spin-labeled Ca^{2+}-ATP and the remaining 31.6% of the intensity arose from MSL-labeled glycoprotein.

EPR analysis of the spin labeled SR

(1) Conventional EPR. The conventional EPR spectrum of the MSL bound to the SR (MSL-SR) is shown in Fig. 2. The spectrum had two components – a predominantly broad component, indicative of strongly immobilized probes (μs time-scale motion) and a minor narrow resonance, indicative of weakly immobilized probes (ns time-scale motion). Computer subtraction of the weakly immobilized signal [36] and double integration of the resulting spectrum showed that the mole percent of strongly immobilized probes (at 4° C) was $97.6 \pm 0.5\%$. Since the spectrum was dominated by labels rigidly attached to the protein, it was interpreted as reliably reporting the motions of the MSL-SR proteins rather than reporting the independent motion of the spin labels in their microenvironments. The values of the outer hyperfine splitting, $2T_{\parallel}'$, and the half-width at half-height of the low-field peak, Δ_L, were 71.3 ± 0.1 gauss and 3.55 ± 0.05 gauss, respectively, and these spectral parameters remained stable as long as the sample was held at 4° C.

(2) Saturation transfer EPR. The ST-EPR spectrum of MSL-SR is shown in Fig. 2. The spectrum was representative of the approx. 97% strongly immobilized spin labels, but contained a more pronounced spectral contribution from the nearly 3% weakly immobilized probes. The rotational correlation time of a spin-labeled protein is commonly deduced from the low-field lineheight ratio, L''/L, in the ST-EPR spectrum. However, the presence of 3% weakly immobilized probes in the sample introduced considerable deformity of the L'' peak, preventing estimation of τ_r from this ratio. Instead, rotational correlation times were obtained from the V_2' H''/H lineheight ratio, which has been shown to be unaffected by the presence of weakly immobilized probes [36].

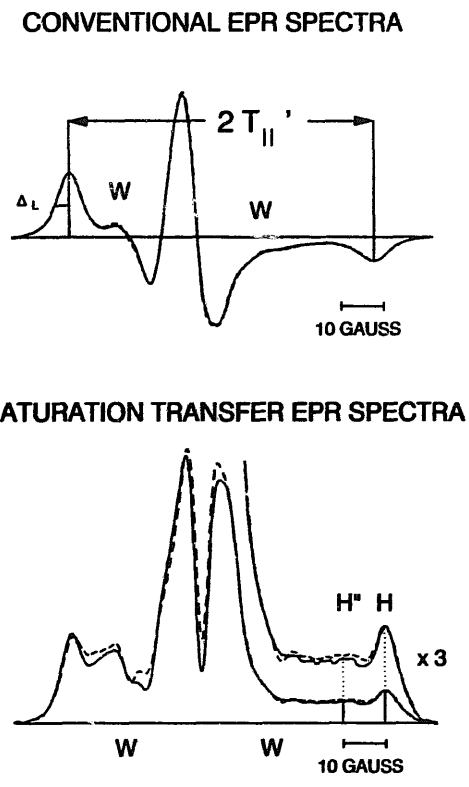

Fig. 2. Conventional and ST-EPR spectra of maleimide spin-labeled SR (MSL-SR) preincubated alone (control, solid line) and with anti-GP-53 antiserum (dashed line) at 4°C. Samples were 50 mg MSL-SR/ml in 0.1 M KCl, 500 μM $CaCl_2$, 20 mM Mops (pH 7.0). Conventional spectra were characterized by the outer splitting, $2T_{\parallel}'$, the half-width at half-height of the low-field peak, Δ_L, and the mole percent of weakly immobilized probes, W. ST-EPR spectra were characterized by the high-field lineheight ratio, H''/H, yielding the effective rotational correlation time, τ_r, by comparison of this ratio to a standard curve as described in Methods. The high-field region of the ST-EPR spectra is shown enlarged by a factor of three to demonstrate the antiserum-induced spectral change in this region. This change, while small, was statistically significant (see Methods) and reproducible. Spectra represent 100 gauss scan range and were collected as described in Methods.

Effect of anti-GP-53 antiserum on the rotational motion of MSL-labeled proteins of SR

The conventional V_1 spectra obtained at 4°C of MSL-SR preincubated with anti-GP-53 antiserum (dashed line, Fig. 2) or with preimmune serum (not shown) were nearly identical to the V_1 spectrum of control MSL-SR. The spectral parameter values of the maximum hyperfine splitting, $2T_{\parallel}'$ (71.4 ± 0.1 gauss (anti GP-53 antiserum) and 71.4 ± 0.1 gauss (preimmune serum)), the half-width at half-height of the low-field peak, Δ_L (3.55 ± 0.05 gauss (antiserum) and 3.62 ± 0.06 gauss (preimmune serum)), and the mole percent of weaky immobilized probes, W (3% for each spectrum), were equivalent to the corresponding values for the control MSL-SR spectrum (Table I). These results indicate that there were no changes in the spin label microenvironment caused by preincubation with either anti-GP-53 antiserum or preimmune serum. Therefore, any differences observed in the rotational motion of the MSL-SR proteins upon binding of antibodies to GP-53 were indicative of changes induced by antibody binding, as opposed to changes in motions of MSL in its microenvironments.

The saturation transfer V_2' spectrum obtained at 4°C of MSL-SR incubated with anti-GP-53 antiserum (Fig. 2, dashed lines) was sensitive to the binding of the antibodies, indicated by a greater than 1.5-fold increase in the effective rotational correlation time of the MSL-SR proteins ($\Delta\tau_r \approx 70$ μs relative to control MSL-SR), as evidenced by the high-field lineheight ratio (control: $H''/H = 0.53 \pm 0.02$, $\tau_r = 128 \pm 26$ μs; antiserum: $H''/H = 0.58 \pm 0.02$, $\tau_r = 202 \pm 64$ μs). The V_2' spectrum obtained at 4°C of MSL-SR incubated with preimmune serum (not shown) was unaffected ($H''/H = 0.55 \pm 0.03$, $\tau_r = 154 \pm 58$ μs). Together, these results suggest that the binding of the antibodies to the GP-53 alone was responsible for the slowed protein rotation.

The antiserum-induced changes in the MSL-SR saturation transfer V_2' spectrum were greatly enhanced when the spectrum was recorded at 20°C. As shown in Fig. 3, increasing amounts of antiserum incubated with MSL-SR induced a greater than 5-fold increase in the effective rotational correlation time of the MSL-SR proteins, consistent with progressive binding of antibodies and concomitant inhibition of MSL-SR protein rotation. Control spectra obtained at 25°C of MSL-SR titrated with preimmune serum showed no effect on MSL-SR protein rotational motion, again suggesting that the rotational motions of the MSL-SR proteins were retarded by the binding of antibodies directed against GP-53.

Kutchai and Campbell [14] found that the ability of the anti-GP-53 antiserum to inhibit active Ca^{2+} uptake

TABLE I

Conventional EPR spectral parameters obtained from MSL-SR at 4°C after incubation with antibodies in the presence [a] and absence [b] of calcium

Parameter	$2T_{\parallel}'$ (gauss) [c]		Δ_L (gauss) [d]		N [e]
Environment	$+Ca^{2+}$	$-Ca^{2+}$	$+Ca^{2+}$	$-Ca^{2+}$	$\pm Ca^{2+}$
Control	71.1±0.2	71.5±0.2	3.6±0.05	3.6±0.05	3
Antiserum	71.5±0.2	71.4±0.1	3.6±0.05	3.6±0.05	5
Preimmune serum	71.4±0.1	71.3±0.1	3.5±0.01	3.6±0.05	3
XB52	71.4±0.2	71.5±0.2	3.6±0.05	3.7±0.10	4
VIIID12	71.3±0.1	71.6±0.1	3.4±0.05	3.5±0.05	1

[a] Antibody incubation buffer and EPR resuspension buffer contained 500 μM $CaCl_2$.

[b] Antibody incubation buffer and EPR resuspension buffer contained 5 mM EGTA.

[c] Outer hyperfine splitting measured as in Fig. 2.

[d] Half-width at half-height of the low-field peak measured as in Fig. 2.

[e] Number of experimental repetitions. Errors listed are standard deviations except for VIIID12, which is a standard measurement error.

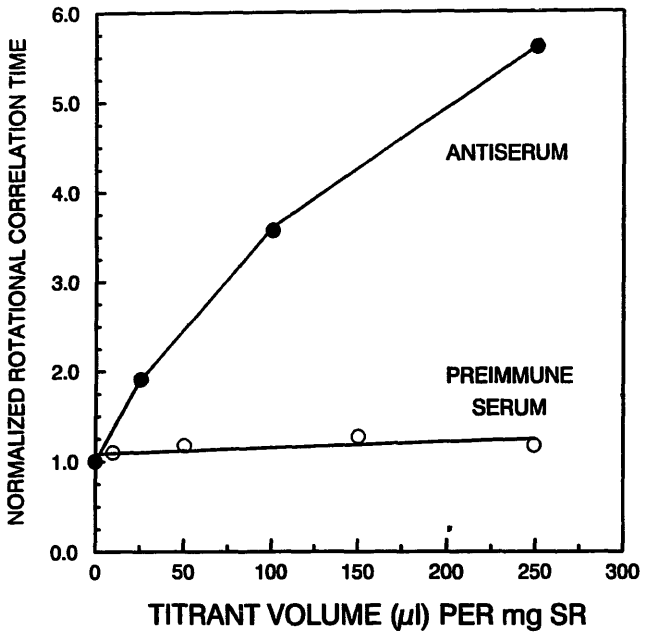

Fig. 3. Effect of antiserum on the effective rotational correlation time of maleimide spin-labeled SR proteins relative to control MSL-SR, measured at 20°C. MSL-SR (2 mg/ml) was incubated with the specified volumes of antiserum per mg of MSL-SR (filled circles) for two hours at 4°C in 0.1 M KCl, 100 μM $CaCl_2$, 20 mM Mops (pH 7.0), final volume 1 ml. As a control, MSL-SR was similarly incubated with increasing volumes of preimmune serum per mg of MSL-SR (open circles). The preincubated MSL-SR was removed from the incubation mixture by a single centrifugation, and the pellet was resuspended in 0.1 mM KCl, 100 μM $CaCl_2$, 20 mM Mops (pH 7.0) for EPR. The effective rotational correlation time for each sample was obtained from the high-field lineheight ratio, H''/H, in the saturation transfer EPR spectrum. Plotted rotational correlation times were normalized by dividing each value by that corresponding to the control value. Typically, the effective rotational correlation time for control MSL-SR at 25°C was 30 ± 5 μs.

by the SR depended strongly on the ratio of antiserum to SR protein in the preincubation period: a ratio of 1 μl antiserum/μg SR protein produced about a 50% inhibition of transport. In this study the ratio of anti-GP-53 antiserum to SR protein required to cause a 2-fold increase in the apparent τ_r of MSL-labeled SR was only 1/10 of that value. Thus monitoring the rotational mobility of MSL-labeled SR proteins provides a much more sensitive indicator of the interaction of anti-GP-53 antibodies with the SR membrane than does measuring active Ca^{2+} transport.

Effect of monoclonal antibodies against GP-53 on the rotational motion of MSL-labeled SR proteins

The conventional V_1 spectra obtained at 4°C of MSL-SR incubated with an anti-GP-53 monoclonal antibody, XB52, and with a control monoclonal antibody, VIIID12 (directed against calsequestrin), were also nearly identical to the V_1 spectrum of control MSL-SR. The 4°C spectra of MSL-SR incubated with the monoclonal antibodies contained no significant differences in the spectral parameters $2T'_{\parallel}$ (71.2 ± 0.1 gauss (XB52) and 71.3 ± 0.1 gauss (VIIID12)), Δ_L (3.6 ± 0.05 gauss (XB52) and 3.55 ± 0.5 (VIIID12)), or W (3% each spectrum), as a function of antibody binding, indicating the spin-label binding environments were not perturbed by antibody binding (Table I).

The saturation transfer V'_2 spectra obtained at 4°C for MSL-SR incubated with XB52 were sensitive to the binding of the monoclonal antibody as indicated by the greater than 2-fold increase in the effective rotational correlation time of the MSL-SR proteins ($\Delta\tau_r \approx 115$ μs relative to control MSL-SR) as evidenced by the high-field lineheight parameter ($H''/H = 0.60 \pm 0.01$, $\tau_r = 243 \pm 43$ μs). The V'_2 spectrum of MSL-SR incubated with VIIID12 showed no effect on the high-field ratio ($H''/H = 0.52 \pm 0.2$, $\tau_r = 117 \pm 11$ μs). Consistent with the antiserum study above, these results suggest that the binding of XB52 to the GP-53 alone was responsible for the slowed protein rotation.

As above, the MAb-induced changes in the MSL-SR saturation transfer spectrum were greatly enhanced when the spectrum was recorded at 20°C. As shown in Fig. 4, increasing amounts of XB52 incubated with MSL-SR resulted in an increase in the effective rotational correlation time of the MSL-SR proteins as indicated by a 4-fold increase in the effective rotational correlation time of MSL-SR proteins compared to control MSL-SR, consistent with progressive binding of XB52 and concomitant inhibition of MSL-SR protein rotation. Control measurements of MSL-SR titrated with VIIID12 showed no effect on MSL-SR protein rotational motion, again suggesting that the rotational motions of the MSL-SR proteins were retarded by the binding of monoclonal antibodies directed against GP-53. We are continuing to investigate the temperature dependence of the effect of both the anti-GP-53 antiserum and MAbs on the rotational motion of the MSL-SR proteins.

Calcium-dependence of the effects of antibodies on the rotational motion of MSL-labeled SR proteins

Having observed that anti-GP-53 antibodies retarded the rotational motion of the MSL-labeled SR proteins, we then investigated the influence of calcium on this effect.

A. Optimization of time of preincubation with antibodies

For each antibody system, optimal antibody binding conditions (i.e., those conditions which would produce consistent and stable antibody-induced changes in the V'_2 spectrum of MSL-SR) were selected. This was accomplished by incubating MSL-SR in a fixed volume of antibody (10 μl) for various lengths of time while monitoring the change in effective rotational correlation time of the MSL-SR proteins. For example, the effect of

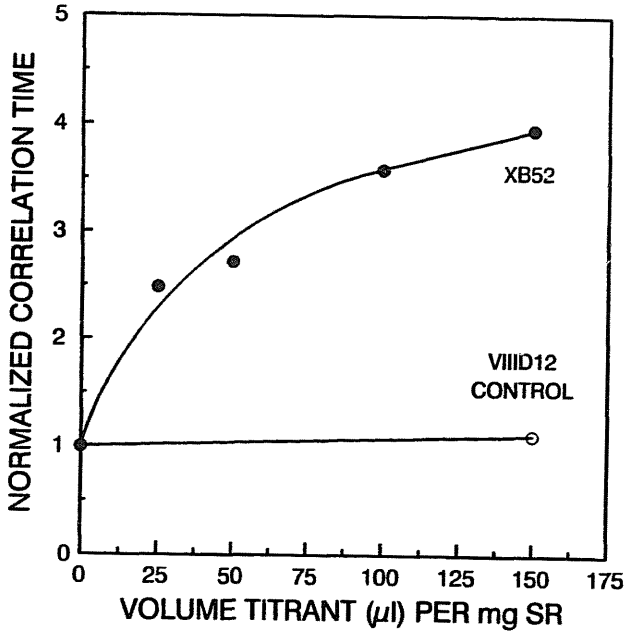

Fig. 4. Effect of monoclonal antibody XB52 (against GP-53) on the effective rotational correlation time of maleimide spin-labeled SR proteins relative to control MSL-SR, measured at 20°C. MSL-SR (2 mg/ml) was incubated with the specified volumes of XB52 per mg of MSL-SR (filled circles) for two hours at 4°C in 0.1 M KCl, 100 μM $CaCl_2$, 20 mM Mops (pH 7.0), final volume 1 ml. As a control, MSL-SR was similarly incubated with the specified volumes of a monoclonal antibody against calsequestrin, VIIID12, per mg of MSL-SR (open circles), which does not cross react with either Ca^{2+}-ATPase or GP-53. The preincubated MSL-SR was removed from the incubation mixture by a single centrifugation, and the pellet was resuspened in 0.1 M KCl, 100 μM $CaCl_2$, 20 mM Mops (pH 7.0) for EPR. The effective rotational correlation time for each sample was obtained from the high-field lineheight ratio, H''/H, in the saturation transfer EPR spectrum. Plotted rotational correlation times were normalized by dividing each value by that corresponding to the control value. Typically, the effective rotational correlation time for control MSL-SR at 25°C was 30 ± 5 μs.

incubating MSL-SR with 10 μl anti-GP-53 antiserum as a function of time on the MSL-SR V_2' spectrum at 4°C is shown in Fig. 5. Quantification of the maximum change in MSL-SR rotation showed a stable, 25% increase in the H''/H lineheight ratio (corresponding to a 2-fold increase in the rotational correlation time) over the control for incubation times of 18 h or longer. Therefore, for the anti-GP-53 antiserum measurements, MSL-SR was incubated with the antibodies for 18 h at 4°C either in the presence (5 mM $CaCl_2$) or absence of calcium (5 mM EGTA). Similar binding curves were measured for XB52, VIE8, and VIIID12 (data not shown) and the optimal preincubation times were selected.

B. Conventional and ST-EPR measurements

(1). Control preparations. Conventional EPR spectra of control MSL-SR samples suspended in the presence and absence of Ca^{2+} and (1) preincubated alone, (2) preincubated with preimmune serum, and (3) preincubated with VIIID12 showed no calcium-dependent changes in the V_1 spectral parameters, $2T_{\parallel}'$, Δ_L, and W (Table I). The rotational correlation times of the MSL-SR proteins in these incubations showed only a small calcium dependence, being slightly shorter in the presence of calcium (Table II).

(2) MSL-SR preincubated with antibodies against GP-53. Similar to the control MSL-SR samples, the conventional EPR spectra of MSL-SR samples suspended in the presence and absence of Ca^{2+} and (1) incubated with anti-GP-53 antiserum and (2) incubated with XB52 showed no calcium-dependent changes in the values of $2T_{\parallel}'$, Δ_L, and W (Table I). However, the effect of anti-GP-53 antibodies (antiserum and XB52) on the rotational motion of the MSL-labeled SR proteins displayed a large calcium-dependence (Table II). For the SR preincubated with anti-GP-53 antiserum, the rotational motion of the MSL-labeled SR proteins, determined by the H''/H lineheight ratio, was about 62 μs slower in the presence of Ca^{2+} than in EGTA ($\tau_r = 202 \pm 64$ μs and 140 ± 81 μs, respectively, a 1.4-fold calcium effect). For SR preincubated with anti-GP-

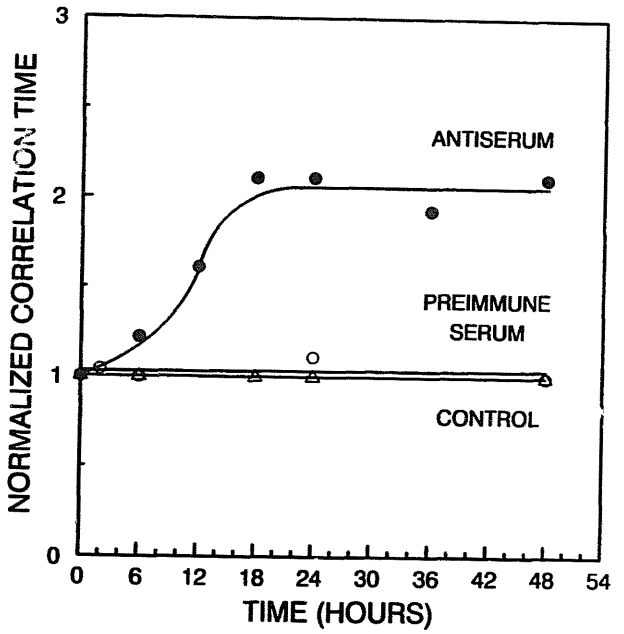

Fig. 5. Time-course of inhibition of MSL-SR protein rotational motion upon preincubation with anti-GP-53 antiserum relative to control MSL-SR, measured at 4°C. MSL-SR (2 mg/ml) was incubated with 10 μl antiserum (open circles) per mg SR at in 0.1 M KCl, 100 μM $CaCl_2$, 20 mM Mops (pH 7.0), final volume 1 ml, for the times indicated at 4°C. Control measurements consisted of similar incubations of MSL-SR either alone (open circles) or with 10 μl preimmune serum (open triangles) per mg SR. The preincubated MSL-SR was removed from the incubation mixture by a single centrifugation, and the pellet was resuspended in 0.1 M KCl, 100 μM $CaCl_2$, 20 mM Mops (pH 7.0) for EPR. The effective rotational correlation time for each sample was obtained from the high-field lineheight ratio, H''/H, in the saturation transfer EPR spectrum. Plotted rotational correlation times were normalized by dividing each value by that corresponding to the control value. Typically, the effective rotational correlation time for control MSL-SR at 4°C was 128 ± 26 μs.

TABLE II

Saturation transfer EPR spectral parameters obtained from MSL-SR at 4°C after incubation with antibodies in the presence [a] and absence [b] of calcium

Environment	H''/H [c]		τ_r (μs) [d]		N [e]
	$+Ca^{2+}$	$-Ca^{2+}$	$+Ca^{2+}$	$-Ca^{2+}$	$\pm Ca^{2+}$
Control	0.53±0.02	0.55±0.03	128±26	154±48	3
Antiserum	0.58±0.02	0.54±0.05	202±64	140±81	5
Preimmune serum	0.55±0.03	0.57±0.03	154±48	185±17	3
XB52	0.60±0.01	0.56±0.01	243±43	169±16	4
VIIID12	0.52±0.02	0.52±0.02	117±11	117±11	1

[a] Antibody incubation buffer and EPR resuspension buffer contained 500 μM $CaCl_2$.
[b] Antibody incubation buffer and EPR resuspension buffer contained 5 mM EGTA.
[c] High-field lineheight ratio measured as in Fig. 5.
[d] Rotational correlation time derived from H''/H using standard plot in Fig. 2.
[e] Number of experimental repetitions. Errors listed are standard deviations except for VIIID12, which is a standard measurement error.

53 monoclonal antibody, XB52, the H''/H lineheight ratios indicated the MSL-labeled proteins also rotated more slowly in a Ca^{2+} environment than in the EGTA environment ($\tau_r = 243 \pm 43$ μs and 169 ± 16 μs, respectively, also a 1.4-fold calcium effect).

Effect of monoclonal antibodies against the Ca^{2+}-ATPase on the rotational motion of MSL-labeled SR proteins

Finding that antibodies directed against GP-53 affected the rotational motion of MSL-SR proteins, we also investigated the effect of a monoclonal antibody against the Ca^{2+}-ATPase, VIE8, on the rotational motion of the MSL-SR proteins. The V_1 spectrum of MSL-SR incubated in the presence of VIE8 showed no significant change from the control MSL-SR spectrum, determined by the spectral parameters $2T'_{\parallel}$ (71.5 ± 0.1 gauss), Δ_L (3.5 ± 0.05 gauss), and W (3%). Analysis of the VIE8-MSL-SR system by ST-EPR showed only a slight slowing of the MSL-SR protein rotational motion upon the binding of VIE8 ($H''/H = 0.55 \pm 0.02$, $\tau_r = 154 \pm 31$ μs).

The fact that the anti-Ca^{2+}-ATPase antibody had virtually no effect on the rotational motion of the MSL-SR suggested that either (a) the antibody was unable to crosslink adjacent single Ca^{2+}-ATPase polypeptides or (b) the antibody successfully crosslinked adjacent Ca^{2+}-ATPase polypeptides, but these single Ca^{2+}-ATPases were already aggregated into oligomers. Kutchai and Campbell [14] and Molnar et al. [41] have demonstrated the ability of VIE8 to successfully bind to the Ca^{2+}-ATPase. This suggests that the VIE8 incubated with MSL-SR bound to an aggregated Ca^{2+}-ATPase. This proposal is consistent with the findings of Birmachu and Thomas [42] who recently reported that at 4°C the Ca^{2+}-ATPase rotates in the SR membrane in an aggregated (oligomeric) form. Having incubated our MSL-SR samples with VIE8 at 4°C, it is reasonable to conclude that these antibodies bound to an aggregated Ca^{2+}-ATPase.

The finding that VIE8 had no effect on the rotational mobility of the Ca^{2+}-ATPase is also consistent with the results of Molnar et al. [41] and Kutchai et al. [43]. Molnar et al. [41] found that although VIE8 bound to SR at room temperature, it had no effect on Ca^{2+}-ATPase activity or calcium uptake by SR. Kutchai et al. [43] also found that incubation of SR with VIE8 at room temperature for several hours had no effect on Ca^{2+}-ATPase activity or Ca^{2+} uptake by the SR. However, when SR was incubated with VIE8 at 37°C, there was a marked inhibition of both Ca^{2+}-ATPase activity and Ca^{2+} uptake. These findings, which are also consistent with the temperature-dependent Ca^{2+}-ATPase aggregation state reported by Birmachu and Thomas [42], suggest that further ST-EPR measurements of MSL-SR rotation at higher temperatures (≥ 25°C) are required to adequately describe the correlation between VIE8-induced changes in Ca^{2+}-ATPase activity/Ca^{2+} uptake and VIE8-induced changes in Ca^{2+}-ATPase rotational motion.

To determine if the interaction of VIE8 with MSL-SR was Ca^{2+}-dependent, MSL-SR was preincubated with VIE6 in the presence and absence of Ca^{2+}. There were no significant changes in the V_1 spectral parameters based on similar values of $2T'_{\parallel}$, Δ_L, and W (Table I). The rotational correlation time of the VIE8-MSL-SR showed only a slight calcium dependence, $\tau_r = 154 \pm 14$ μs in 5 mM $CaCl_2$ and 128 ± 12 μs in 5 mM EGTA (1.2-fold calcium effect). This result was consistent with the finding, described above, that the binding of VIE8 to MSL-SR had little effect on the rotational motions of the MSL-labeled SR proteins.

Interpretation of changes of rotational times observed

Since we found that both Ca^{2+}-ATPase and GP-53 contained bound MSL, it is difficult to know whether our experimental results are due to immobilization of GP-53 alone by the anti-GP-53 antibodies or whether there is evidence for retardation of the rotational mobility of Ca^{2+}-ATPase as well. Since (a) more of the MSL label is on the Ca^{2+}-ATPase than on GP-53 and (b) there were increases in the effective rotational correlation time of the MSL-SR proteins greater than 5- and 4-fold as a function of antiserum and XB52 binding to SR, respectively, it is worthwhile to inquire whether the increases observed in τ_r can be accounted for by changes in the mobility of GP-53 alone.

We approached this issue by doing V'_2 spectral intensity parameter simulations. Intensity parameters were selected because the total intensity of a two component V'_2 spectrum (where each component displays μs rota-

tion) is a linear combination of the individual intensities of the two components. (This does not hold true for the H''/H parameter.) Since it is not possible to know the extent to which the polyclonal antibodies crosslink GP-53, we modeled the experiments involving XB52, the MAb against GP-53. Since an MAb recognizes only one epitope on the antigen, the most that XB52 can do is to crosslink all the GP-53 present in the membrane into units of two GP-53 molecules. This would be expected to double the rotational correlation time of GP-53 (see Discussion) [44]. Having found that 1.3 mol of MSL was bound per mol of Ca^{2+}-ATPase and 0.9 mol MSL bound per mol of GP-53 in our MSL-SR preparations (described above) and using the mole ratio of GP-53 : Ca^{2+}-ATPase in the SR membrane of 2 : 3 [17], we assumed that the intensity parameter of MSL-Ca^{2+}-ATPase alone constituted 68.4% of the final simulated intensity parameter while the intensity parameter of MSL-GP-53 constituted the remaining 31.6% of the final simulated intensity parameter. In our simulations we tried to include the range of reasonable values for the rotational correlation times of Ca^{2+}-ATPase and GP-53. We used values of τ_r of Ca^{2+}-ATPase of 50 and 100 μs, which are similar to values previously reported [40,45]. We chose values of τ_r for GP-53 before being crosslinked by MAb of 1, 10, and 100 μs, which we believe cover the range of possible values for this protein. Our calculations assumed that crosslinking by XB52 is 100% efficient and the rotational correlation time of all GP-53 present doubled upon XB52 binding.

The rotational correlation times chosen for the simulations were converted to intensity parameters using an MSL-Hb intensity parameter standard curve (not shown, see Ref. 36) similar to the high-field lineheight ratio standard curve described in the Methods. Using various linear combinations of the derived V_2' intensity parameters for GP-53 and Ca^{2+}-ATPase alone, weighted as described above, the expected V_2' intensity parameters for GP-53 and Ca^{2+}-ATPase together were generated. From the predicted intensity parameters, predicted values of τ_r were generated via the standard curve for comparison with our experimental results.

The results of the simulations are shown in Table III. The simulations predict that at most we should have observed a 15% increase in observed apparent τ_r. As shown in Table II, we observed an approx. 200% increase in apparent τ_r for MSL-SR preincubated with the monoclonal antibody against GP-53 compared with a control preincubated with a monoclonal antibody against calsequestrin, an intraluminal protein of the SR. It is interesting to note that if the molar ratio of GP-53 : Ca^{2+}-ATPase was even as high as 1 : 1 (which is clearly an overestimate of the amout of GP-53 in the membrane), then we should have observed at most a 52% increase in τ_r (deduced from similar calculations, not shown). This suggests that preincubation with XB52 caused decreased rotational mobility of Ca^{2+}-ATPase as well as GP-53 and is consistent with the interpretation that there is interaction between GP-53 and Ca^{2+}-ATPase in the SR membrane.

TABLE III

Results of spectral simulations to investigate the possible effects of monoclonal antibody XB52 on the observed rotational correlation time of MSL-SR proteins [a]

τ_r, Ca^{2+}-ATPase	τ_r (μs)				% increase in apparent τ_r
	assumed τ_r, GP-53		predicted apparent τ_r of MSL-SR		
	−MAb	+MAb	−MAb	+MAb	
50	1	2	28	28	0
	10	20	35	38	8
	100	200	67	77	14
100	1	2	34	36	5
	10	20	44	48	9
	100	200	100	115	15

[a] The MAb is assumed to crosslink all GP-53 present into dimers, thus doubling the τ_r of GP-53. Spectral simulations were done using the ratio of GP-53:Ca^{2+}-ATPase of 2:3 [17] with 1.3 mol of MSL/mol Ca^{2+}-ATPase and 0.9 mol MSL/mol GP-53 (see text). Rotational correlation times are in μs.

Discussion

Overview

Four previous studies support the interpretation that there is a functional interaction between Ca^{2+}-ATPase and GP-53 in the SR membrane. Chiesi and Carafoli [15] reported that trifluoperazine binds to GP-53 and, as a result, produces a decrease in the affinity of the Ca^{2+}-ATPase for Ca^{2+}. Leonards and Kutchai [16] extracted GP-53 from SR membranes and found a correlation between the amount of GP-53 that remained and the ability of the SR to actively accumulate Ca^{2+}. Kutchai and Campbell [14] reported that an anti-GP-53 antiserum can uncouple Ca^{2+} transport from ATP hydrolysis. Boyd et al. [12] found that when GP-53 was perturbed, either by partial extraction with detergent or with anti-GP-53 antiserum, the cooperativity of the dependence of Ca^{2+}-ATPase activity on [Ca^{2+}] and [ATP] was diminished. The only evidence against a functional interaction between GP-53 and Ca^{2+}-ATPase was provided by Leberer et al. [20], who found that endoplasmic reticulum isolated from COS-1 cells transfected with the cDNA for Ca^{2+}-ATPase alone transported Ca^{2+} just as well as cells co-transfected with the cDNAs for Ca^{2+}-ATPase and GP-53.

In planning the present study, we reasoned that if there is a stable interaction between Ca^{2+}-ATPase and GP-53 in the SR membrane, then retarding the mobility of GP-53 should diminish the mobility of the Ca^{2+}-ATPase. Antibodies against GP-53 were used to cross-

link GP-53, and we asked whether this affected the rotational mobility of spin-labeled Ca^{2+}-ATPase.

The results described above show that antibodies against GP-53, either a polyclonal antiserum or monoclonal antibodies, can retard the rotational mobility of spin-labeled SR proteins. The retarding effects of the anti-GP-53 antibodies on the rotational rate of SR proteins is diminished in the absence of Ca^{2+}. In the case of the anti-GP-53 monoclonal antibody (XB52), model calculations suggest that the binding of antibodies results in retarding the mobility of Ca^{2+}-ATPase, as well as slowing the motion of GP-53.

The effect of anti-GP-53 antibodies on rotational mobility of SR proteins

At the outset of this work, it was our intention to use a reproducible spin-labeling method that would label only the Ca^{2+}-ATPase on a single sulfhydryl residue per Ca^{2+}-ATPase in a highly immobilized environment in order to allow us to observe the rotational motion of the Ca^{2+}-ATPase exclusively. This would have enabled us to monitor the rotational motion of the Ca^{2+}-ATPase in the presence and absence of anti-GP-53 antibodies to determine if there is a physical interaction between GP-53 and the Ca^{2+}-ATPase in the SR membrane.

The experimental rationale was as follows: An anti-GP-53 antibody, having two antigen binding sites, will effectively serve to crosslink two GP-53 polypeptides upon binding. The effect of crosslinking GP-53 on the rotational motion of the Ca^{2+}-ATPase would have two extreme cases: (1) if GP-53 has no interaction with the Ca^{2+}-ATPase, such that the rotational correlation time measured for the Ca^{2+}-ATPase reflects only the rotation of the Ca^{2+}-ATPase, itself, then increasing the molecular mass of the glycoprotein via antibody crosslinking would have no effect on the rotational motion of the Ca^{2+}-ATPase (though it is possible that clustering GP-53 might increase the rotational rate of Ca^{2+}-ATPase), or (2) if GP-53 were to have a physical interaction with the Ca^{2+}-ATPase, then increasing the effective molecular mass of the glycoprotein via antibody crosslinking would show a marked effect on the rotational motion of the Ca^{2+}-ATPase.

The method we used to spin label SR, however, did not result in MSL bound exclusively to the Ca^{2+}-ATPase. While the use of *N*-ethylmaleimide (NEM) prelabeling might have insured exclusive labeling of the Ca^{2+}-ATPase [40], we found that it had a detrimental effect on the Ca^{2+} uptake activity of the SR, preventing correlation of the observed changes in rotational mobility of SR proteins caused by anti-GP-53 antibodies with changes in Ca^{2+} transport due to anti-GP-53 antibodies that were previously observed [14]. Therefore, due to the presence of bound spin label on GP-53 in our MSL-SR preparations, the results described above cannot be interpreted exclusively in terms of MSL-Ca^{2+}-ATPase rotational motion.

Interpretation of observed changes in rotational correlation times

Experiments with anti-GP-53 antiserum. Since both Ca^{2+}-ATPase and GP-53 are labeled with MSL, interpretation of observed changes in apparent rotational correlation times is not straightforward. While ST-EPR spectra give information about protein rotation on the μs timescale, they do not contain direct information about the nature of the rotating species [46]. However, it is still useful to monitor changes in observed rotational correlation times, even when the exact physical significance of these correlation times is unclear.

The polyclonal antibodies in the anti-GP-53 antiserum have multiple epitopes. The antiserum thus has the potential to crosslink GP-53 into quite large aggregate of many individual GP-53 molecules. We do not know the size of the aggregate of GP-53 formed by preincubation with antiserum under the conditions of our experiments. For that reason the observed increases in rotational correlation time in the presence of anti-GP-53 antiserum are difficult to interpret.

While we are unable to quantify the changes observed in rotational correlation time after preincubation with anti-GP-53 antiserum in terms of a physical model of the rotating species, a general conclusion is possible: The observed slowing of rotational motion of the MSL-labeled SR proteins is due to binding of antibodies to GP-53 exclusively since GP-53 is the only target of the anti-GP-53 antibodies. Saffman and Delbrük [44] have shown that the rotational diffusion of an integral membrane protein, occurring primarily about an axis parallel to the membrane normal, is inversely proportional to the molecular radius of the rotating unit and the viscosity of the surrounding medium. Because membrane viscosity is far greater than that of the aqueous phase surrounding the membrane, the rotation of the protein is governed only by the molecular mass within the membrane and is virtually independent of the mass of protein in the aqueous phase. When individual GP-53 polypeptides are crosslinked by an antibody, they become one rotating unit with an increased effective size of the intramembranous segment of the rotating unit. The increase in size is determined by the extent of crosslinking by the antibodies. Thus, the expected result of crosslinking GP-53 is slowed GP-53 rotation. Our finding that GP-53 rotation slowed upon antibody binding is consistent with an increase in the size of the rotating unit via 'crosslinking' of GP-53 molecules by the antibodies present in the anti-GP-53 antiserum.

Since there is such a large change in apparent rotational correlation time after preincubation with anti-GP-53 antiserum, and since far more of the MSL is bound to Ca^{2+}-ATPase than to GP-53, it is tempting to

speculate that the motion of Ca^{2+}-ATPase is also being diminished by the anti-GP-53 antibodies.

Experiments with monoclonal anti-GP-53 antibodies. Since monoclonal antibodies recognize a single epitope on the antigen, MAbs against GP-53 can only crosslink two GP-53 molecules. For this reason it is possible to make plausible assumptions about the effect of an anti-GP-53 MAb on the size of the GP-53 unit that rotates in the SR membrane. In the model calculations described above, we assumed that preincubation with the anti-GP-53 MAb XB52 results in doubling the average rotational correlation time of GP-53. The results of our model calculations (Table III) show that the largest increase in apparent rotational correlation time that could result from doubling the rotational correlation time of GP-53 is 15%. We observed an increase of approx. 200% in the apparent rotational correlation time after preincubation with MAb XB52 (Table II).

Even with the extreme assumptions of 100% crosslinking efficiency inducing a doubling of τ_r for all GP-53 molecules, the model calculations suggest that the maximum effect of MAb XB52 in retarding the mobility of GP-53 is not sufficient to account for so large an increase as we observed in the experimental apparent τ_r. The simplest explanation for this discrepancy is that preincubation with the anti-GP-53 MAb also results in profoundly slowing the rotational mobility of the other MSL-labeled protein species, the Ca^{2+}-ATPase. This is consistent with the interpretation that there is a physical interaction between GP-53 and Ca^{2+}-ATPase in the SR membrane.

Ca^{2+}-dependence of the effect of anti-GP-53 antibodies

As described above, we found that the immobilization of MSL-labeled SR proteins by anti-GP-53 antibodies was considerably greater in the presence of Ca^{2+} (0.5 mM) than in the absence of Ca^{2+}. One interpretation of this result is that the interaction between Ca^{2+}-ATPase and GP-53 is enhanced by the presence of Ca^{2+}. We are continuing to study the dependence of this effect on Ca^{2+} concentration, which must be more fully characterized before we can speculate on its possible physiological significance.

Conclusion

This study provides evidence that supports the following conclusions: (1) binding of anti-GP-53 antibodies to SR vesicles results in slowing the rotational mobility of GP-53 and probably of Ca^{2+}-ATPase as well. This suggests an interaction between GP-53 and Ca^{2+}-ATPase; and (2) the interaction between GP-53 and Ca^{2+}-ATPase appears to be enhanced by the presence of Ca^{2+}.

Additional study is needed to more completely characterize the nature of the interactions between GP-53 and Ca^{2+}-ATPase and to elucidate its possible physiological significance. Studies with SR membranes whose Ca^{2+}-ATPase is specifically labeled with a phosphorescent probe have the potential to characterize more precisely the effects reported here. One of us (J.E.M.) is currently involved in such studies in David Thomas' Laboratory at the University of Minnesota.

Acknowledgments

J.E.M. and C.M.G. were supported by National Institutes of Health Research Grant AM19419, a grant from the Muscular Dystrophy Association of America, and a grant from the National Science Foundation. The EPR instrumentation used in these studies was provided by grants from the National Science Foundation and the University of Virginia. C.P.W. was supported by Training Grant T32HL07284 from the National Institutes of Health. H.K. was supported by a Grant-in-Aid from the American Heart Association, Virginia Affiliate. We are grateful to Dr. David H. MacLennan, University of Toronto, for providing anti-GP-53 antiserum and preimmune serum and to Dr. Kevin P. Campbell, University of Iowa, for providing monoclonal antibodies XB52, VIE8, and VIIID12. We thank Dr. David D. Thomas, University of Minnesota, for providing the TPX sample capillary and holder, the peak fitting software, and for his advice on data analysis. We thank Dr. Thomas C. Squier, University of Kansas, for his assistance in training us in the proper execution of ST-EPR experiments, and for his comments on the manuscript.

References

1 De Meis, L. (1981) in The Sarcoplasmic Reticulum (Bittar, E.E., ed.) pp. 1–6, John Wiley and Sons, New York.
2 MacLennan, D.H. (1970) J. Biol. Chem. 245, 4508–4518.
3 Michalak, M. (1985) in Enzymes of Biological Membranes (Martonosi, A.N., ed.), Vol. 3, pp. 115–153, Plenum Press, New York.
4 Ikemoto, N. (1982) Annu. Rev. Physiol. 44, 297–317.
5 Inesi, G. (1985) Annu. Rev. Physiol. 47, 573–601.
6 Ikemoto, N., Garcia, A.M., Kurobe, Y. and Scott, T.L. (1983) J. Biol. Chem. 256, 8593–8601.
7 Froehlich, J.P. and Heller, P.F. (1985) Biochemistry 24, 126–136.
8 Napier, R.M., East, J.M. and Lee, A.G. (1987) Biochim. Biophys. Acta 903, 365–373.
9 Napier, R.M., East, J.M. and Lee, A.G. (1987) Biochim. Biophys. Acta 903, 374–380.
10 Squier, T.C., Hughes, S.E. and Thomas, D.D. (1988) J. Biol. Chem. 263, 9162–9170.
11 Squier, T.C. and Thomas, D.D. (1988) J. Biol. Chem. 263, 9171–9177.
12 Boyd, K.L., Xu, Q., Weis, C.P. and Kutchai, H. (1989) Biophys. J. 55, 481a.
13 Tada, M., Yamada, M., Inui, M. and Ohmori, F. (1982) Mol. Cell Biochem. 46, 73–95.
14 Kutchai, H. and Campbell, K.P. (1989) Biochemistry 28, 4830–4839.

15 Chiesi, M. and Carafoli, E. (1982) J. Biol. Chem. 257, 984–991.
16 Leonards, K.S. and Kutchai, H. (1985) Biochemistry 24, 4876–4884.
17 Michalak, M., Campbell, K.P. and MacLennan, D.H. (1980) J. Biol. Chem. 255, 1317–1326.
18 Pepper, D.R., Raab, C.R. and Campbell, K.P. (1985) Biophys. J. 47, 344a.
19 Campbell, K.P. and MacLennan, D.H. (1981) J. Biol. Chem. 256, 4626–4632.
20 Leberer, E., Charuk, J.H.M., Clarke, D.M., Green, N.M., Zubrzycka-Gaarn, E. and MacLennan, D.H. (1989) J. Biol. Chem. 264, 3484–3493.
21 Campbell, K.P. and MacLennan, D.H. (1983) J. Biol. Chem. 258, 1391–1394.
22 Repke, D.I., Spivak, J.C. and Katz, A.M. (1976) J. Biol. Chem. 251, 3169–3175.
23 Eletr, S. and Inesi, G. (1972) Biochim. Biophys. Acta 282, 174–197.
24 Madden, T.D., Chapman, D. and Quinn, P.J. (1979) Nature (London) 279, 538–541.
25 Martonosi, A. and Ferretos, R. (1964) J. Biol. Chem. 239, 648–658.
26 Lowry, O.H., Rosebrough, N.J., Farr, A.L. and Randall, R.J. (1951) J. Biol. Chem. 193, 265–275.
27 Yamada, S. and Ikemoto, N. (1978) J. Biol. Chem. 253, 6801–6807.
28 Griffith, O.H. and McConnell, H.M. (1966) Proc. Natl. Acad. Sci. USA 55, 8–11.
29 Laemmli, U.K. (1970) Nature (London) 227, 680–685.
30 Campbell, K.P. and MacLennan, D.H. (1982) J. Biol. Chem. 257, 1238–1246.
31 Campbell, K.P., Knudson, C.M., Imagawa, T., Leung, A.T., Sutko, J.L., Kahl, S.D., Raab, C.R. and Madson, L. (1987) J. Biol. Chem. 262, 6460–6463.
32 Hemminga, M.A., Reinders, J.H. and DeJager, P.A. (1984) J. Magn. Res. 58, 428–441.
33 Popp, C.A. and Hyde, J.S., (1981) J. Magn. Res. 43, 249–258.
34 Hemminga, M.A., DeJager, P.A., Marsh, D. and Fajer, P. (1984) J. Magn. Res. 59, 160–163.
35 Thomas, D.D., Dalton, L.R. and Hyde, J.S. (1976) J. Chem. Phys. 65, 3006–3024.
36 Squier, T.C. and Thomas, D.D. (1986) Biophys. J. 49, 921–936.
37 Morse, P.D. (1987) Biophys. J. 51, 440a.
38 Segur, J.B. and Oberstar, H.E. (1951) Ind. Eng. Chem. 43, 2117–2120.
39 Thomas, D.D. and Hidalgo, C. (1978) Proc. Natl. Acad. Sci. USA 75, 5488–5492.
40 Hidalgo, C. and Thomas, D.D. (1977) Biochem. Biophys. Res. Commun. 78, 1175–1182.
41 Molnar, E., Seidler, N.W., Jona, I. and Martonosi, A.N. (1990) Biochim. Biophys. Acta 1023, 147–167.
42 Birmachu, W. and Thomas, D.D. (1990) Biochemistry 29, 3904–3914.
43 Kutchai, H., Geddis, L.M. and Campbell, K.P. (1990) Biophys. J. 57, 500a.
44 Saffman, P.J. and Delbrük, M. (1975) Proc. Natl. Acad. Sci. U.S.A. 72, 3111–3113.
45 Squier, T.C. and Thomas, D.D. (1986) Biophys. J. 49, 937–942.
46 Thomas, D.D. (1986) in Techniques for the Analysis of Membrane Proteins (Ragan, C.I. and Cherry, R.J., eds.) pp. 377–431, Chapman and Hall, London.